

# Simultaneously Multiply-Configurable or Superposed Molecular Logic Systems Composed of ICT (Internal Charge Transfer) Chromophores and Fluorophores Integrated with One- or Two-Ion Receptors

A. Prasanna de Silva\* and Nathan D. McClenaghan\*[a]

**Abstract:** Integrated “ICT chromophore–receptor” systems show ion-induced shifts in their electronic absorption spectra. The wavelength of observation can be used to reversibly configure the system to any of the four logic operations permissible with a single input (YES, NOT, PASS 1, PASS 0), under conditions of ion input and transmittance output. We demonstrate these with dyes integrated into Tsien’s calcium receptor, **1–2**. Applying multiple ion inputs to **1–2** also allows us to perform two- or three-input OR or NOR operations. The weak fluorescence output of **1** also shows YES or NOT logic depend-

ing on how it is configured by excitation and emission wavelengths. Integrated “receptor<sub>1</sub>–ICT chromophore–receptor<sub>2</sub>” systems **3–5** selectively target two ions into the receptor terminals. The ion-induced transmittance output of **3–5** can also be configured via wavelength to illustrate several logic types including, most importantly, XOR. The opposite effects of the two ions on the energy of the chromophore excited state is re-

**Keywords:** fluorescence • molecular logic gates • molecular switches • UV/Vis spectroscopy

sponsible for this behaviour. INHIBIT and REVERSE IMPLICATION are two of the other logic types seen here. Integration of XOR logic with a preceding OR operation can be arranged by using three ion inputs. The fluorescence output of these systems can be configured via wavelength to display INHIBIT or NOR logic under two-input conditions. The superposition or multiplicity of logic gate configurations is an unusual consequence of the ability to simultaneously observe multiple wavelengths.

## Introduction

Molecular logic,<sup>[1]</sup> a sub-discipline within the area of molecular-level devices and machines,<sup>[2]</sup> had been a recurring dream since the 80s.<sup>[3]</sup> There was an example in the conference literature based on light input–light output,<sup>[4]</sup> but this was not followed up with a detailed report in the primary literature to clarify its mechanism of action. Logic operations as advanced as parallel processing of numbers were accomplished by Wild<sup>[5]</sup> but the molecules so used had no intrinsic logic capability. The first example of intrinsically molecular logic in the primary literature involved chemical-induced fluorescence switching.<sup>[6]</sup>

Readiness for operation in the single molecule regime,<sup>[7]</sup> simplicity of the “fluorophore–spacer–receptor” modular design,<sup>[8]</sup> essential completeness of the fluorescence switching phenomenon<sup>[9]</sup> are some of the reasons for the rapid uptake of this and related approaches<sup>[10–16]</sup> in the drive towards ever more complex molecular logic systems. Many of these are

wireless photoionic systems utilising ionic inputs, a photonic output and a photonic power supply. By way of comparison, electronic approaches to molecular-scale logic have problems of communication with the macro domain which are not easy to overcome,<sup>[17]</sup> though molecule populations with switching properties have been conventionally wired with bulk metal contacts to produce OR logic gates.<sup>[18]</sup> Even a bundle of carbon nanotubes have been treated to show NOT logic recently.<sup>[19]</sup> The all-photonic approach to molecular-scale logic has recently begun to bear fruit.<sup>[16]</sup>

The principle of chemical-induced optical switching has been unequivocally established by focussing on systems which give essentially “off/on” switching of light signals across the entire visible spectrum.<sup>[6]</sup> Once this has been done, we can look at more complicated systems which require more careful definition of wavelength for their operation. We now show that ion-induced transmittance changes displayed by integrated “chromophore–receptor” systems can be a useful approach to molecular logic. Transmittance output is a less sensitive means of detecting molecules than the fluorescence approach,<sup>[20, 21]</sup> though modulation techniques allow some movement towards the single molecule regime.<sup>[22]</sup> Sacrifice of modularity is necessarily a complication, but even some understanding of integrated systems can allow us to unveil

[a] Prof. Dr. A. P. de Silva, Dr. N. D. McClenaghan  
School of Chemistry, Queen’s University  
Belfast BT9 5AG (Northern Ireland)  
Fax: (+44) 2890-382117  
E-mail: a.desilva@qub.ac.uk, n.mc-clenaghan@lcoo.u-bordeaux.fr

interesting logic phenomena which have not been seen with modular systems (see below). Another impetus for this work is the available wealth of integrated “chromophore–receptor” systems within the classical literature of chemical indicators,<sup>[23]</sup> reagents,<sup>[24]</sup> general chemical equilibria<sup>[25]</sup> and supramolecular chemistry<sup>[26]</sup> which can now be interpreted and exploited for logic purposes.

## Results and Discussion

The molecules developed for the current study incorporate independent receptor sites for the biologically relevant  $\text{Ca}^{2+}$  or other Group II ions (**1–5**), and protons (**3–5**) and operate in aqueous media. Some measurements are conducted at pH 7.2 and ionic strength 0.1M (KCl) for physiological relevance.<sup>[27]</sup> The design format, represented in Figure 1, involves an internal charge transfer (ICT) excited state.<sup>[21]</sup> The receptor site(s) are intimately linked to the chromophore, such that the binding of one (or two) guests perturbs the excited state, with a resulting spectral shift. Molecule **1**, represented schematically in Figure 1a, contains a cyanine-type push-pull chromophore strongly coupled to the modified EGTA-type receptor introduced by Tsien for intracellular studies.<sup>[27]</sup> Several related structures containing crown receptors are known.<sup>[28]</sup> **1–5** are metallochromic chromophore/lumophores at physiological pH values (and ionic strength).

The tetramethyl ester **6**<sup>[29]</sup> served as a precursor for **1a** to **5a**. Syntheses of **1a** and **2a**, as the tetramethyl esters, were achieved by condensation reactions<sup>[30]</sup> of aldehyde **6** with 1,4-dimethylpyridinium iodide<sup>[31]</sup> (or 1,4-dimethylquinolinium iodide<sup>[31]</sup>) in alcoholic solution, with piperidine as the base. Acid hydrolysis then yielded the target molecules **1** or **2**. Molecules **3a–5a** were prepared by benzoyl chloride catalysed coupling<sup>[32]</sup> of **6** with 4-methylpyridine, 4-methylquinoline or 9-methylacridine,<sup>[33]</sup> respectively. Subsequent base hydrolysis then gave **3–5**.

The response of **1** to  $\text{Ca}^{2+}$  is shown for illustrative purposes in Figure 2, with a nett blue-shifting of the low-energy absorption band relative to that of the guest-free species, reflecting the ion-induced destabilisation of the ICT-excited state (Figure 1a). This results from a combination of loss of resonance (as the electrons of the anilinic nitrogen are involved in

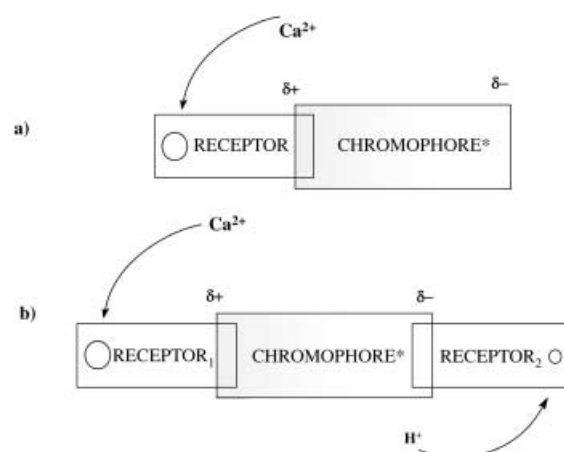


Figure 1. Schematic representation of ICT excited states of **1** and **2** (a), and **3–5** (b). In each case the receptor site(s) are strongly coupled with the chromophore.

binding the guest<sup>[34]</sup>) and an electrostatic repulsion between the guest and the adjacent developed  $\delta+$  charge. Qualitatively similar spectral shifts are observed for other Group II metal ions,  $\text{Sr}^{2+}$  and  $\text{Ba}^{2+}$  (with relatively small variations in the energy corresponding to the  $\lambda_{\text{Abs}}$  values, which are linearly related to the ionic radius of the guest in accordance with earlier findings on related structures<sup>[28]</sup>). The collected optical and binding properties for **1–5** are listed in Table 1.

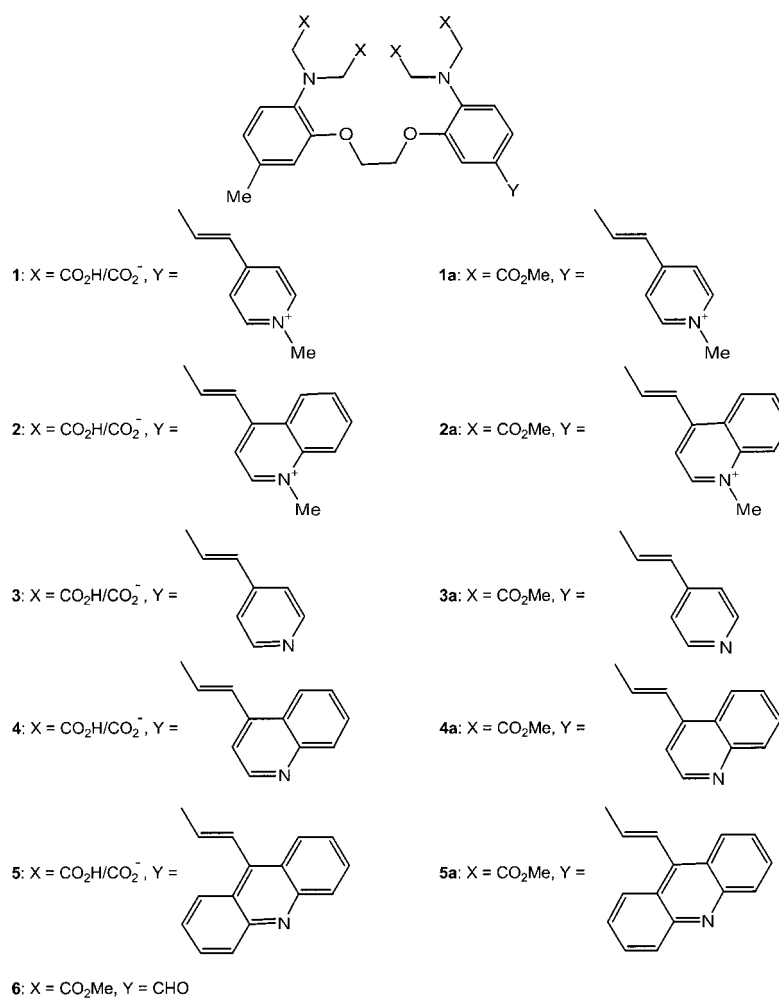


Table 1. Optical and binding properties of **1–5** with different Group II ions and protons.<sup>[a,b]</sup>

Species	$\lambda_{\text{Abs}}$ ( $\epsilon_{\text{max}}$ ) nm ( $\text{M}^{-1}\text{cm}^{-1}$ )	Destabilisation [kJ mol <sup>-1</sup> ]	$\log\beta^{[\text{c}]}$
<b>1</b>	444 (19800)	–	–
<b>1</b> ·Ca <sup>2+</sup>	372 (20300)	53	5.9
<b>1</b> ·Sr <sup>2+</sup>	378 (19600)	48	4.7
<b>1</b> ·Ba <sup>2+</sup>	384 (18000)	42	5.5
<b>1</b> ·H <sup>+</sup>	427 (16700)	11	5.8
<b>2</b>	505 (10600)	–	–
<b>2</b> ·Ca <sup>2+</sup>	406 (10500)	58	6.3
<b>2</b> ·Sr <sup>2+</sup>	413 (10000)	53	4.8
<b>2</b> ·Ba <sup>2+</sup>	420 (9900)	48	5.5
<b>2</b> ·H <sup>+</sup>	490 (7500)	7	5.8
<b>3</b> <sup>[d]</sup>	372 (22000)	–	–
<b>3</b> ·H <sup>+</sup>	436 (21000) <sup>[e]</sup>	–48 <sup>[e]</sup>	7.1 (6.8) <sup>[f]</sup>
<b>3</b> ·Ca <sup>2+</sup> <sup>[d]</sup>	330 (24000)	41	6.2
<b>3</b> ·Ca <sup>2+</sup> ·H <sup>+</sup>	365 (22000) <sup>[e]</sup>	6 <sup>[e]</sup>	<sup>[g]</sup>
<b>4</b> <sup>[d]</sup>	394 (13000)	–	–
<b>4</b> ·H <sup>+</sup>	478 (12000) <sup>[e]</sup>	–54 <sup>[e]</sup>	7.0 (6.6) <sup>[f]</sup>
<b>4</b> ·Ca <sup>2+</sup> <sup>[d]</sup>	347 (14000)	41	6.1
<b>4</b> ·Ca <sup>2+</sup> ·H <sup>+</sup>	396 (14000) <sup>[e]</sup>	–1 <sup>[e]</sup>	<sup>[h]</sup>
<b>4</b> ·Sr <sup>2+</sup> <sup>[d]</sup>	350 (14200)	38	5.8
<b>4</b> ·Sr <sup>2+</sup> ·H <sup>+</sup>	401 (10400) <sup>[e]</sup>	–5 <sup>[e]</sup>	<sup>[i]</sup>
<b>4</b> ·Ba <sup>2+</sup> <sup>[d]</sup>	354 (15000)	34	5.8
<b>4</b> ·Ba <sup>2+</sup> ·H <sup>+</sup>	407 (10700) <sup>[e]</sup>	–10 <sup>[e]</sup>	<sup>[j]</sup>
<b>5</b> <sup>[d]</sup>	426 (8800)	–	–
<b>5</b> ·H <sup>+</sup>	533 (14800) <sup>[e]</sup>	–57 <sup>[e]</sup>	7.0 (10.3) <sup>[f]</sup>
<b>5</b> ·Ca <sup>2+</sup> <sup>[d]</sup>	395 (9700)	22	6.4
<b>5</b> ·Ca <sup>2+</sup> ·H <sup>+</sup>	444 (8500) <sup>[e]</sup>	–12 <sup>[e]</sup>	<sup>[k]</sup>

[a]  $\approx 10^{-5}$  M **1–5** in H<sub>2</sub>O at room temperature, pH 7.2 throughout unless otherwise noted. The concentrations were chosen to give reasonable absorbance values at  $\lambda_{\text{Abs}}$ . [b] The fluorescence emission wavelengths (quantum yields) [ $\lambda_{\text{Flu}}$  ( $\phi_{\text{F}}$ )] for **1**, **1**·Ca<sup>2+</sup>, **1**·Sr<sup>2+</sup>, **1**·Ba<sup>2+</sup>, **4** and **4**·Ca<sup>2+</sup> are 591 ( $1 \times 10^{-4}$ ), 554 ( $5 \times 10^{-4}$ ), 563 ( $3 \times 10^{-4}$ ), 575 ( $2 \times 10^{-4}$ ), 569 ( $7 \times 10^{-4}$ ) and 540 ( $2 \times 10^{-3}$ ), respectively. The fluorescence quantum yields for **4**·H<sup>+</sup> and **4**·Ca<sup>2+</sup>·H<sup>+</sup> are both  $< 1 \times 10^{-4}$ . [c] Binding constants ( $\beta$ ) determined from the variation of absorbance ( $A$ ) with ion concentration ( $m$ ) according to the mass action-type equation  $\log[(A_{\text{max}} - A)/(A - A_{\text{min}})] = -\text{p}m - \log\beta$ .<sup>[35]</sup> A similar determination is done for fluorescence intensity variations. All binding constants reported are conditional formation constants for the conditions stated. Besides their intrinsic interest, these also aid discussion on logic operations. The reciprocal of the binding constant represents the threshold of the chemical input level at which switching of the optical output level is caused. [d] pH 9.5. [e] pH 5.4. [f] Value obtained by fluorescence measurements. [g]  $\log\beta_{\text{Ca}^{2+}} = 5.0$  (pH 6.0),  $\log\beta_{\text{Ca}^{2+}} = 6.1$  [pH 7.2, ionic strength 0.1M (KCl)],  $\log\beta_{\text{H}^{+}} = 6.5$  (pCa 2.3),  $\log\beta_{\text{H}^{+}}$  (by fluorescence measurements) = 6.8 (pCa 2.3). [h]  $\log\beta_{\text{Ca}^{2+}} = 6.0$  (pH 6.0),  $\log\beta_{\text{Ca}^{2+}} = 6.6$  [pH 7.2, ionic strength 0.1M (KCl)],  $\log\beta_{\text{H}^{+}} = 6.4$  (pCa 2.3),  $\log\beta_{\text{H}^{+}}$  (by fluorescence measurements) = 6.2 (pCa 2.3). [i]  $\log\beta_{\text{Sr}^{2+}} = 3.9$  (pH 5.6). [j]  $\log\beta_{\text{Ba}^{2+}} = 4.1$  (pH 5.6). [k]  $\log\beta_{\text{Ca}^{2+}} = 5.4$  (pH 6.0),  $\log\beta_{\text{Ca}^{2+}} = 6.7$  [pH 7.2, ionic strength 0.1M (KCl)],  $\log\beta_{\text{H}^{+}} = 6.3$  (pCa 2.3),  $\log\beta_{\text{H}^{+}}$  (by fluorescence measurements) = 10.4 (pCa 2.3).

It is also evident from Table 1 that incorporation of an additional fused ring to the chromophore (**2** as compared to **1**, for instance) has the effect of significantly red-shifting the absorption bands due the greater electron delocalisation, thus allowing a degree of tuning of the chromophore properties. These molecules also serve as models for the more complex second class of molecules represented by **3–5** (see below).

#### Multiple logic configurations of **1–2** in transmittance mode:

If the metal ion-induced blue-shift of **1** and **2** is large enough, there will be some (long) wavelengths where the transmittance is switched “off-on” and some (short) wavelengths

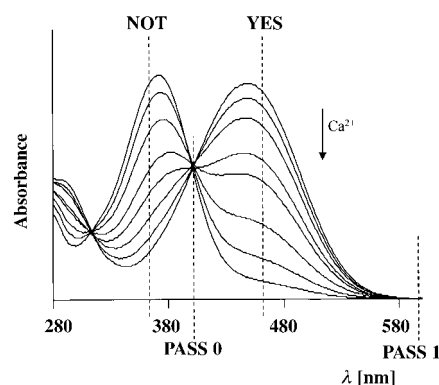


Figure 2. Absorption spectra of **1** with varying pCa, showing YES, NOT, PASS 0 and PASS 1 logic. pCa values in order of increasing absorbance at 470 nm; 2.3, 5.2, 5.7, 6.0, 6.2, 6.5, 7.0,  $\infty$ . [General conditions given in the footnotes to Table 1 apply throughout unless otherwise noted. Ionic strength (KCl) = 0.1].

where it is switched “on-off” at the same time. Thus, opposite switching actions can be displayed by one molecular system being observed at two different wavelengths. In terms of molecular logic, utilising one ionic input for example Ca<sup>2+</sup> and a transmittance output, YES(PASS) and NOT logic can be demonstrated upon monitoring at the appropriate wavelength (462 and 363 nm, respectively for **1**). YES logic is obtained when a high input gives a high output; and a low input gives a low output; while NOT logic corresponds to an inversion of YES logic. Monitoring at the isosbestic point (401 nm) gives a low transmittance value irrespective of the ionic input present and thus corresponds to the PASS 0. The final possible logic expression that can be produced with a one-input gate is the PASS 1. This can be obtained upon monitoring at 595 nm, where a high transmittance output results regardless of the input condition. Though the last two logic types are considered to be trivial in electronics textbooks,<sup>[36]</sup> we believe it is important that all four possible single-input logic configurations have been achieved by simple experiments with **1**. Fluorescence excitation spectra of the celebrated calcium sensor fura-2<sup>[29]</sup> for example give a somewhat similar result though with higher sensitivity of signal detection. Once we are armed with this interpretation, many pH and metallochromic indicators<sup>[23]</sup> can be seen to exhibit these four logic types. This means that a large body of data now becomes available for this type of analysis. The truth tables with operational parameters are shown within Table 2. Importantly, these gates (unlike electronic devices) are able to exhibit all four possible logic operations simultaneously upon monitoring at the appropriate wavelengths. At this point it is appropriate to remember the observation of particulate or wave-like behaviour from a small object depends on the experiment performed. This is the textbook duality of quantum systems. The related effect of superposition exists in quantum computation, where quantum bit strings can exist simultaneously in all possible states.<sup>[37]</sup> It is to be noted, however, that superposition here applies to the quantum bits rather than to the logic gates. In the present instance, we are seeing different logic gate types depending on the observation wavelength used. This can therefore be described as the simultaneous multiplicity or

Table 2. Truth tables showing simultaneous multiplicity of logic gate configurations (YES, NOT, PASS 0, PASS 1) for **1**: transmittance output.<sup>[a]</sup>

Input Ca <sup>2+</sup>	Output			
	YES <sub>462 nm</sub>	NOT <sub>363 nm</sub>	PASS 0 <sub>401 nm</sub>	PASS 1 <sub>595 nm</sub>
0	0 (low, 1 <sup>[b]</sup> )	1 (high, 35 <sup>[b]</sup> )	0 (low, 5 <sup>[b]</sup> )	1 (high, 100 <sup>[b]</sup> )
1	1 (high, 68 <sup>[b]</sup> )	0 (low, 1 <sup>[b]</sup> )	0 (low, 5 <sup>[b]</sup> )	1 (high, 100 <sup>[b]</sup> )

[a] 0 and 1 are digital representations of low and high signal levels respectively throughout. The low and high input levels of Ca<sup>2+</sup> correspond to <math>10^{-9}</math>M and <math>10^{-2.3}</math>M, respectively, in all discussions unless otherwise noted. [b] % transmittance at the stated wavelengths for 10 cm optical path length throughout.

superposition of photoionic logic systems, a feature apparently unavailable in textbooks on electronic logic systems.<sup>[36]</sup>

As far as we can see, reconfiguring logic gates in an electronics context is a serial process where a particular stimulus changes the logic operation from one to another. The electronically programmable read only memory (EPROM) is one such example among several in the electronics field.<sup>[36, 38]</sup> For a mixed electronics-molecular example of non-simultaneous reconfiguring, see ref. [18]. Somewhat related examples are also known where an ionic,<sup>[15a]</sup> electrochemical<sup>[39]</sup> or photochemical<sup>[40]</sup> stimulus alters a sensory selectivity of a molecular system. These latter cases can be viewed as “off-on” switches, that is YES logic gates in which the output response to a chosen input is being altered without changing the logic operation itself. In all these cases, whether electronics- or chemical-based, there is only one given logic operation at a given time. However, it is easy to simultaneously observe multiple wavelengths since this is what we do during colour vision. Optical multi-channel analyzers or even beam-splitters and filters would permit the same parallel operation on the photonic output of **1–5**. Thus the simultaneous multiplicity or superposition of photoionic logic gates becomes possible, that is where a given molecular system serves as more than one logic gate at the one time simply by observing at different wavelengths. This opens interesting perspectives, when we remember the revolution in data communications caused by the move from metal to fibre-optic lines where the multiplex opportunities offered by light were unavailable with electric voltages. However, multiplexing in an electronic logic gate context has a very different meaning.<sup>[36]</sup> The closest electronics analogy to the chemical phenomenon under discussion is perhaps found in multi-gate chip packages which will give different logic outputs from different pins.<sup>[36]</sup>

Previous chemical examples of switching actions which depend on observation wavelength are in references [14, 15b, 41–46]. Some of these references specifically refer to logic operations. References [13, 15a] consider logic operations which depend upon a different external variable, the pH value. Additionally, in the present (and subsequent) examples, an inversion of each of these operations is possible by coding for an absorbance rather than a transmittance output. Thus, if a YES operation was demonstrated through a transmittance output, a NOT operation would result from an absorbance output. Nevertheless, we shall maintain the transmittance coding so that all instances of significantly large light emanation from the sample (whether by trans-

mittance or by luminescence) will be consistently taken as output logic state 1. We note in passing that conventional electronic systems also have the choice of positive or negative logic with the former being the more common.<sup>[36]</sup>

**YES/NOT logic operations with **1** in fluorescence mode:** YES and NOT logic can also be expressed through a weak fluorescence output with **1** (**2** is significantly less emissive), as shown in Figure 3 and Table 3. The ion-induced absorption spectral shifts allow the choice of excitation wavelength to

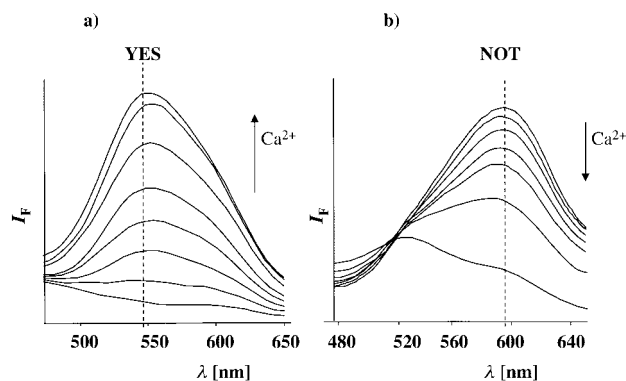


Figure 3. Fluorescence spectra of **1** with varying pCa, showing a) YES logic on exciting at 372 nm (pCa values in order of decreasing intensity at 548 nm; 2.3, 4.9, 5.7, 6.0, 6.5, 7.0, 7.5,  $\infty$ ) and b) NOT logic on exciting at 454 nm (pCa values in order of increasing intensity at 591 nm; 2.3, 6.0, 6.5, 7.0, 7.5, 8.0,  $\infty$ ). [Ionic strength (KCl) = 0.1].

Table 3. YES and NOT logic with **1**: fluorescence output.<sup>[a]</sup>

Input Ca <sup>2+</sup>	Output	
	YES <sub>548 nm</sub> excited at 372 nm	NOT <sub>591 nm</sub> excited at 454 nm
0	0 (low, 7 <sup>[b]</sup> , $5 \times 10^{-5}$ <sup>[c]</sup> )	1 (high, 100 <sup>[b]</sup> , $3 \times 10^{-4}$ <sup>[c]</sup> )
1	1 (high, 100 <sup>[b]</sup> , $5 \times 10^{-4}$ <sup>[c]</sup> )	0 (low, 25 <sup>[b]</sup> , $1 \times 10^{-4}$ <sup>[c]</sup> )

[a] Output given as fluorescence emission at the stated wavelengths of excitation and emission. [b] Intensity in arbitrary units. [c] Fluorescence quantum yield.

maximise the fluorescence switching action desired. A recent example of this strategy can be seen in ref. [47]. A PASS 0 can also be demonstrated by employing relatively long wavelengths. The multiplicity of clearly definable logic gate configurations in the fluorescence mode is smaller than with transmittance in this instance. Though we note that the availability of two parameters for optimisation (excitation and emission wavelengths) should allow easier demonstration of higher multiplicities in adequately fluorescent cases. However, dissimilar fluorescence spectral variations with different guest ions prohibits the demonstration of logic operations involving multiple input channels ( $\phi_F = 5 \times 10^{-4}$  with Ca<sup>2+</sup>,  $3 \times 10^{-4}$  with Sr<sup>2+</sup>,  $2 \times 10^{-4}$  with Ba<sup>2+</sup>) (see later, concerning **4**). In spite of this use of **1** in a logic context, the detailed understanding of ion-induced fluorescence intensity variations in ICT systems such as **1** is still at an embryonic stage.<sup>[48]</sup> We note in passing that systems related to **1** have found use as probes for microviscosity.<sup>[49]</sup>

**Three-input logic with **1–2** in transmittance mode:** Using a transmittance output and multiple ionic inputs yields the OR

(one or more high inputs gives a high output) and NOR (one or more high inputs gives a low output; analogous to a particular integration of an OR and a NOT gate) logic expressions, with the number of possible input channels limited by the number of different guest species eliciting similar responses. In the present instance, the spectral shifts seen with  $\text{Ca}^{2+}$ ,  $\text{Sr}^{2+}$  and  $\text{Ba}^{2+}$  for **1** and **2** are sufficiently similar. Examples of two- and three-input molecular logic gates are obtained utilising different combinations of Group II guest species. OR and NOR logic operations are demonstrated with **1** in Figure 4 for the three-input case (the two-

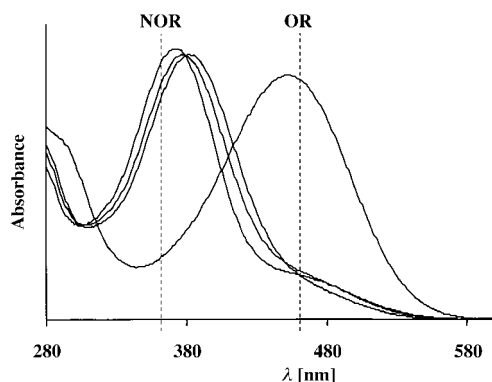


Figure 4. OR and NOR logic with **1**. Ionic inputs in order of increasing absorbance at 363 nm; none,  $\text{Ba}^{2+}$  (pBa 2.3),  $\text{Sr}^{2+}$  (pSr 2.3),  $\text{Ca}^{2+}$  (pCa 2.3).

input case being subsumed into it) whilst Table 4 shows operational parameters. Thus the multiplicity of logic operations is also demonstrated for three-input photoionic systems.

Table 4. Truth tables for OR and NOR logic with **1** using three ionic inputs: transmittance output.

Input <sub>1</sub> $\text{Ca}^{2+}$	Input <sub>2</sub> $\text{Sr}^{2+}$ [a]	Input <sub>3</sub> $\text{Ba}^{2+}$ [a]	Output	
			OR <sub>462 nm</sub>	NOR <sub>363 nm</sub>
0	0	0	0 (low, 1)	1 (high, 34)
0	0	1	1 (high, 48)	0 (low, 2)
0	1	0	1 (high, 44)	0 (low, 2)
1	0	0	1 (high, 46)	0 (low, 2)
0	1	1	1 (high, 47)	0 (low, 1)
1	0	1	1 (high, 47)	0 (low, 1)
1	1	0	1 (high, 46)	0 (low, 1)
1	1	1	1 (high, 46)	0 (low, 2)

[a] The low and high input levels of  $\text{Sr}^{2+}$  and  $\text{Ba}^{2+}$  correspond to  $<10^{-9}\text{M}$  and  $10^{-2.3}\text{M}$ , respectively, in all discussions unless otherwise noted.

**XOR logic with 3–5 in transmittance mode:** A crucial point in this paper is that molecules such as **1** and **2** can be developed into other types of two-input logic systems with small structural modifications. In addition to a metal-ion binding site, **3–5** also incorporate a second receptor site (a heterocyclic nitrogen atom) located within the chromophore, which can be selectively protonated. As shown schematically in Figure 1b, binding  $\text{Ca}^{2+}$  at receptor<sub>1</sub> destabilises the excited state (by  $41\text{ kJ mol}^{-1}$  for **4** relative to the free-species) due the

close proximity of the positively charged guest and the developed  $\delta^+$  charge. Conversely, binding a proton at receptor<sub>2</sub> stabilises the excited state (by  $54\text{ kJ mol}^{-1}$  relative to the guest-free species) with a resulting spectral red-shift. With molecule **4** hosting both guests, these effects are largely equal and opposite. The two different receptors located at opposite poles of the chromophore afford this unprecedented combination of four distinct effects, which in turn can be used to express the XOR logic operation (Table 5). Multiple protonation of related push-pull chromophores provide valuable lessons.<sup>[50]</sup>

Table 5. Truth tables for XOR logic with **3–5**: transmittance output.

Input <sub>1</sub> $\text{Ca}^{2+}$	Input <sub>2</sub> $\text{H}^+$ [a]	Output		
		<b>3</b> XOR <sub>361 nm</sub>	<b>4</b> XOR <sub>387 nm</sub>	<b>5</b> XOR <sub>425 nm</sub>
0	0	0 (low, 15)	0 (low, 16)	0 (low, 47)
0	1	1 (high, 53)	1 (high, 59)	1 (high, 67)
1	0	1 (high, 53)	1 (high, 58)	1 (high, 68)
1	1	0 (low, 17)	0 (low, 15)	0 (low, 47)

[a] The low and high input levels of  $\text{H}^+$  correspond to pH values of 9.7 and 5.6, respectively, in all discussions unless otherwise noted.

The response of **4** to protons in the absence and presence of calcium is shown in Figures 5 and 6, respectively. The values of several parameters for this series (**3–5**), in which an additional fused ring is introduced into the chromophore in

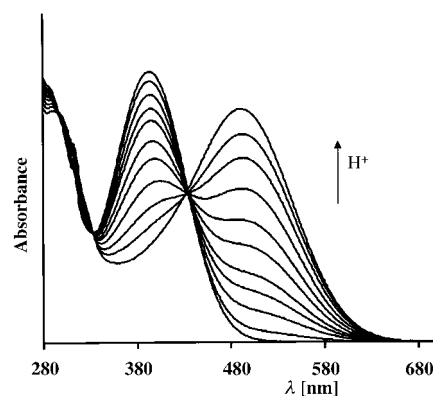


Figure 5. Absorption spectra of **4** with varying pH, in the absence of  $\text{Ca}^{2+}$ . pH values in order of increasing absorbance at 392 nm; 6.4, 6.6, 6.7, 6.9, 7.0, 7.2, 7.3, 7.4, 7.6, 7.8, 9.9.

successive species, is shown in Table 1. In each case the  $\text{p}K_{\text{a}}$  value ( $\log\beta_{\text{H}^+}$ ) is measurable with absorption and fluorescence experiments, at least when  $\text{Ca}^{2+}$  is absent. Significant changes of the  $\text{p}K_{\text{a}}$  value can result upon excitation to an ICT state<sup>[51]</sup> if proton transfer equilibrium is attainable within the excited-state lifetime. The most delocalized system **5** evidently satisfies this condition whereas **3** and **4** do not. In **3–5** the  $\log\beta_{\text{H}^+}$  value in the presence of a  $\text{Ca}^{2+}$  guest is lowered by about 0.6 pH units, as a result of a loss of electron density at the proton receptor. Allosteric effects of this kind are well-appreciated in supramolecular research.<sup>[52]</sup> The inverse case of proton-induced changes of  $\log\beta_{\text{Ca}^{2+}}$  values (Table 1) is also

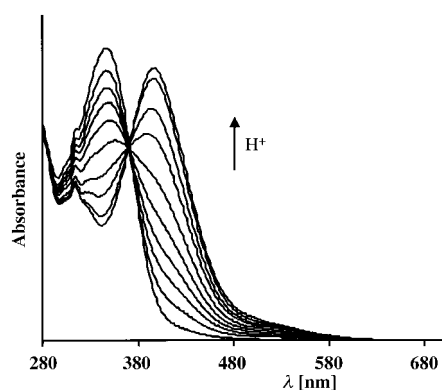


Figure 6. Absorption spectra of **4** with varying pH, in the presence of  $\text{Ca}^{2+}$  ( $10^{-2.3}$  M). pH values in order of increasing absorbance at 392 nm; 9.7, 7.0, 6.8, 6.7, 6.6, 6.4, 6.2, 6.1, 5.8, 5.6.

best discussed at this point. Since protonation of the heterocyclic nitrogens sets in only around pH 7.0 (Table 1) (the protonation of the  $\text{Ca}^{2+}$  receptor does not set in seriously until around pH 6.4<sup>[27]</sup>) the  $\log\beta_{\text{Ca}^{2+}}$  values at pH 9.5 and 7.2 are similar in spite of the high ionic strength employed in the latter case. However the  $\log\beta_{\text{Ca}^{2+}}$  values begin to drop, though by varying amounts in the cases **3–5**, upon going to pH 6.0 even though protonation is incomplete especially in the presence of increasing amounts of  $\text{Ca}^{2+}$ . pH 6.0 was chosen as the high proton input condition for optimal logic behaviour of **3–5** and the corresponding AND gates for half-adder operation.<sup>[53]</sup> The  $\log\beta_{\text{Ca}^{2+}}$  values are expected to fall when the distal heterocyclic nitrogens become protonated because the aniline nitrogens connected to the chromophore become more strongly conjugated. The subsequent flattening of the anilinic moiety alters the spatial position of the acetate arms to give a poorer chelating unit towards a  $\text{Ca}^{2+}$  guest. Interestingly, **5** also has a  $\text{p}K_{\text{a}}$  value ( $\log\beta_{\text{H}^+}$ , Table 1) and long absorption wavelength ( $\epsilon = 3300 \text{ M}^{-1} \text{ cm}^{-1}$  at 650 nm) which are related to structures used in photodynamic therapy of cancerous tissue.<sup>[54]</sup> We note that most of the properties of **4** illustrated here can also be discerned with **3** and **5**.

An XOR gate is one in which the presence of only one high input value registers a high output value. With neither (or both) high inputs present, a low output signal results. Demonstration of XOR logic has proved to be one of the more difficult to implement at the molecular level, with the first case provided by Balzani, Stoddart and co-workers<sup>[55]</sup> utilising the threading/dethreading processes of a pseudorotaxane. Whilst their system expressed the correct truth table (shown in Table 5), it relied upon chemical inputs which annihilate each other, that is acid and base. Therefore each input cannot be recognised simultaneously, which in turn hampers (but does not completely exclude<sup>[45]</sup>) incorporation into a more advanced system, such as parallel operation with a suitable AND gate to yield a molecular half-adder.<sup>[53]</sup> Pina et al. report a more recent case of XOR logic.<sup>[56]</sup> A demonstration of the closely related XNOR logic operation, again involving photoactive pseudorotaxanes,<sup>[57]</sup> required oxidation/reduction potentials as inputs which also annihilate each other.

The optimised situation for **4** is shown in Figure 7 with the observation wavelength being set at 387 nm to extract the

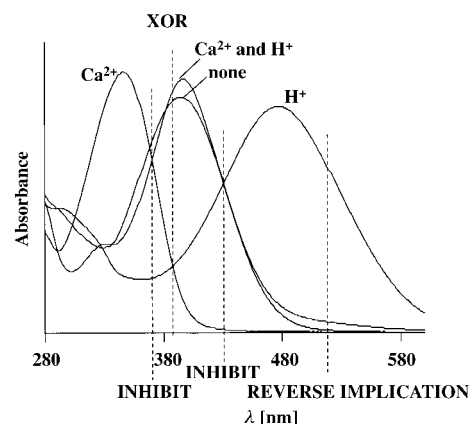


Figure 7. XOR, INHIBIT (two types) and REVERSE IMPLICATION logic with **4**, transmittance observed at 387, 369, 430 and 511 nm.

XOR logic function (Table 5). The ionic inputs are bound at the respective receptor sites giving four different states with formal negative charges of different values  $-1$  ( $\mathbf{4} \cdot \text{Ca}^{2+} \cdot \text{H}^+$ ),  $-2$  ( $\mathbf{4} \cdot \text{Ca}^{2+}$ ),  $-3$  ( $\mathbf{4} \cdot \text{H}^+$ ) or  $-4$  (**4** when free of  $\text{H}^+$  and  $\text{Ca}^{2+}$ ). As each member of this class (**3–5**) demonstrated this particular phenomenon to varying amounts, a certain degree of tuning is clearly allowed by incorporation of additional fused rings. In particular, the operational wavelength to monitor output is adjustable. Other operations displayed by **4** and its cousins utilising a transmittance output, as demonstrated for **1** and **2**, upon choosing the correct restrictions and coding with respect to Figures 5 and 6 are: YES, NOT, PASS 1, PASS 0, OR, NOR. These are not detailed in order to keep the length of the paper within reasonable bounds.

**Additional logic types with 4 in transmittance mode:** While molecules **3–5** were designed principally to produce the XOR logic function, the broadness of their absorption spectra coupled with the relative complexity of their ion-induced shifts permits the emergence of additional logic types at other observation wavelengths. The simultaneous multiplicity of logic configurations is thus seen to be a general phenomenon which applies to two-input photoionic systems as well. The INHIBIT logic function (as described by the truth table within Table 6) occurs if the presence of one high (the disabling)

Table 6. Truth tables for more logic types with **4**: transmittance output.

Input <sub>1</sub> $\text{Ca}^{2+}$	Input <sub>2</sub> $\text{H}^+$	Output		
		INHIBIT <sub>369 nm</sub> <sup>[a]</sup>	INHIBIT <sub>430 nm</sub> <sup>[b]</sup>	REVERSE IMPLICATION <sub>511 nm</sub> <sup>[c]</sup>
0	0	0 (low, 24)	0 (low, 32)	1 (high, 100)
0	1	1 (high, 65)	0 (low, 32)	0 (low, 25)
1	0	0 (low, 25)	1 (high, 96)	1 (high, 100)
1	1	0 (low, 26)	0 (low, 32)	1 (high, 93)

[a] Disabling input:  $\text{Ca}^{2+}$ . [b] Disabling input:  $\text{H}^+$ . [c] Disabling input:  $\text{H}^+$ .

input nullifies the action of the other, with an overall output of 0. In the absence of this disabling input, the other input imposes a YES logic function on the molecule. This can also be profitably viewed as a two-input AND gate, one of whose

input lines contains an inverter. This logic type appears when observations are made at 369 nm and 430 nm. The difference at these two wavelengths is that the disabling input changes over.  $\text{Ca}^{2+}$  is the disabling input in the 369 nm result whereas  $\text{H}^+$  is the disabling input in the 430 nm case. Two-input INHIBIT logic such as this was reported in 2000 by Gunnlaugsson et al.<sup>[11]</sup> The more complex three-input case appeared one year earlier.<sup>[57a]</sup> A more recent case is also available.<sup>[12]</sup> The previously unreported REVERSE IMPLICATION logic shows up when we observe at 511 nm. This logic type, though being also one of the sixteen two-input logic classes, can be represented combinationally as a two-input OR gate, one of whose input lines (input<sub>2</sub>) contains an inverter. Because of the non-commutative nature of this logic operation, declaration of  $\text{H}^+$  as input<sub>1</sub> and  $\text{Ca}^{2+}$  as input<sub>2</sub> would have produced the IMPLICATION logic type instead. Related situations have been recently described.<sup>[13]</sup> Again, it is worth noting that all these logic types can be observed simultaneously if required.

#### Integrated OR and XOR logic with **4** in transmittance mode:

Variation of the inputs such that two different metals are employed, each of which produces a similar response, affords the opportunity to demonstrate the integrated logic situation shown in Figure 8. This is analogous to an integration of OR and XOR gates, where the output of the OR gate serves as an input for the XOR gate. A 2-gate, 3-input and 5-wire situation is represented in Figure 8, with the corresponding truth table

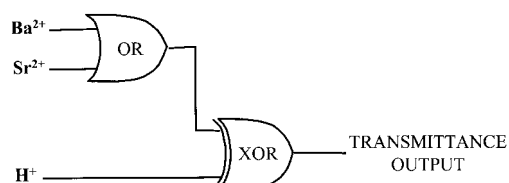


Figure 8. Physical electronic representation of the integration of OR and XOR logic functions within **3–5**: transmittance output.

being shown in Table 7. Coding for  $\text{Sr}^{2+}$  and  $\text{Ba}^{2+}$  inputs (in place of  $\text{Ca}^{2+}$ ) allows an unprecedented demonstration of this operation at the molecular level. Deliberate integration of logic functions within molecules only has a 3-year history.<sup>[58]</sup> As mentioned previously under the OR logic properties of **1**, the  $\lambda_{\text{Abs}}$  differences between  $\mathbf{4} \cdot \text{Sr}^{2+}$  and  $\mathbf{4} \cdot \text{Ba}^{2+}$  (although not as convenient with  $\mathbf{4} \cdot \text{Ca}^{2+}$ ) are small enough to allow this use of **4**. Analysis of the truth table shows discernible XOR and

Table 7. Truth table showing integrated OR and XOR logic with **4**, as shown in Figure 8.

Input <sub>1</sub> $\text{Ba}^{2+}$	Input <sub>2</sub> $\text{Sr}^{2+}$	Input <sub>3</sub> $\text{H}^+$	Output Integrated XOR and OR <sub>402 nm</sub>
0	0	0	0 (low, 3)
0	0	1	1 (high, 25)
0	1	0	1 (high, 56)
1	0	0	1 (high, 43)
0	1	1	0 (low, 5)
1	0	1	0 (low, 5)
1	1	0	1 (high, 48)
1	1	1	0 (low, 5)

OR functions. This means that at a fixed pH value a YES/OR function can be effected using one/different metal cation input(s), in addition to demonstration of the XOR function. Recent cases of integrated molecular logic systems are in refs. [13–15, 58].

**YES/NOT logic with **4** in fluorescence mode:** In addition to the logic operations afforded through a transmittance output, other logic operations can be demonstrated through a fluorescence output. YES logic is obtained as  $\text{Ca}^{2+}$  increases the output fluorescence (at high pH values), whilst NOT logic results from the diminished fluorescence quantum yield on protonation of receptor<sub>2</sub> (in the absence of  $\text{Ca}^{2+}$ ). Both these one-input cases were demonstrated for **1** and **2**, and therefore for brevity, only two-input cases are discussed in the following sections.

**INHIBIT logic with **4** in fluorescence mode:** Molecule **1** was shown to demonstrate YES logic, however, with the additional  $\text{H}^+$  input channel, species **4** has the ability to exhibit the more complex INHIBIT function, via a fluorescence output. This logic expression can be demonstrated with **4** when monitoring the fluorescence output at 510 nm on exciting at the 371 nm quasi-isosbestic point (Figure 6). The absorbances at 371 nm are similarly high for three of the four input conditions, whereas for the fourth [low ( $<10^{-9}\text{M}$ )  $\text{Ca}^{2+}$  and high ( $10^{-5.7}\text{M}$ )  $\text{H}^+$ ] it is greatly decreased. So a low fluorescence is expected for  $\mathbf{4} \cdot \text{H}^+$  due to poor excitation. Figure 9

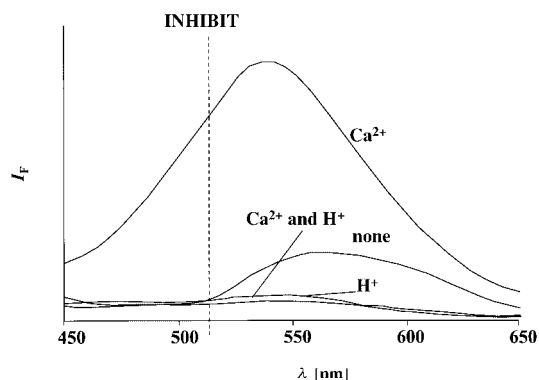


Figure 9. INHIBIT logic with **4** through fluorescence output (excitation at 371 nm and observation at 510 nm).

clearly shows a significant fluorescence band at 570 nm for **4** free of  $\text{H}^+$  and  $\text{Ca}^{2+}$ , but its intensity at the monitoring wavelength of 510 nm is small. The fluorescence efficiency of  $\mathbf{4} \cdot \text{H}^+$  and  $\mathbf{4} \cdot \text{Ca}^{2+} \cdot \text{H}^+$  are likely to be low because of a vibrational-loss mechanism of the protonated species in a protic solvent.<sup>[59]</sup> For  $\text{Ca}^{2+}$ -free species, the formation of a non-emissive twisted internal charge transfer state (TICT)<sup>[60]</sup> and a PET process from the discrete anilinic moiety appear feasible but are evidently not dominant since **4** free of  $\text{H}^+$  and  $\text{Ca}^{2+}$  is clearly emissive. The latter TICT and PET channels would be blocked in the presence of  $\text{Ca}^{2+}$  and so it is reasonable that  $\mathbf{4} \cdot \text{Ca}^{2+}$  shows a strong emission centred at 540 nm with substantial intensity at the monitoring wavelength. Implementation of this logic expression for **4** with the

appropriate excitation and monitoring wavelengths is shown in Figure 9 with a fluorescence enhancement of 11.5 between high and essentially coincident low states. The corresponding truth table can be found within Table 8.

Table 8. Truth tables for INHIBIT and NOR logic with **4**: fluorescence output.<sup>[a]</sup>

Input <sub>1</sub> Ca <sup>2+</sup>	Input <sub>2</sub> H <sup>+</sup>	INHIBIT <sub>510 nm</sub> <sup>[b]</sup> excited at 371 nm	Output NOR <sub>595 nm</sub> excited at 435 nm
0	0	0 (low, 9 <sup>[c]</sup> , 5 × 10 <sup>-4[d]</sup> )	1 (high, 100 <sup>[c]</sup> , 7 × 10 <sup>-4[d]</sup> )
0	1	0 (low, 9 <sup>[c]</sup> , 2 × 10 <sup>-4[d]</sup> )	0 (low, 9 <sup>[c]</sup> , 2 × 10 <sup>-4[d]</sup> )
1	0	1 (high, 100 <sup>[c]</sup> , 2 × 10 <sup>-3[d]</sup> )	0 (low, 9 <sup>[c]</sup> , 2 × 10 <sup>-4[d]</sup> )
1	1	0 (low, 7 <sup>[c]</sup> , 2 × 10 <sup>-4[d]</sup> )	0 (low, 9 <sup>[c]</sup> , 2 × 10 <sup>-4[d]</sup> )

[a] Output given as fluorescence emission at the stated wavelengths of excitation and emission. [b] Disabling input: H<sup>+</sup>. [c] Intensity in arbitrary units. [d] Fluorescence quantum yield.

**NOR logic with **4** in fluorescence mode:** Shifting the wavelength conditions of excitation and observation allows us to address NOR logic with **4**. Previous examples of fluorescent molecular NOR logic gates have utilised a PET mechanism and other processes.<sup>[58]</sup> Molecule **4** also displays this type of logic upon exciting at the 435 nm quasi-isosbestic point (Figure 5), through a combination of effects. Of all four ionic states, **4**·Ca<sup>2+</sup> alone has a diminished absorption at this exciting wavelength and therefore a small fluorescence output. As mentioned above, the protonated species (with or without a Ca<sup>2+</sup> guest) is susceptible to non-radiative vibrational deexcitation in water solvent.<sup>[59]</sup> With neither guest present, we have the significant emission centred at 570 nm. So the fluorescence output at the monitoring wavelength of 595 nm is substantially higher, thus the NOR logic gate is produced. This specific monitoring wavelength produces a coincidentally low emission for the species **4**·Ca<sup>2+</sup>·H<sup>+</sup>, **4**·Ca<sup>2+</sup> and **4**·H<sup>+</sup>. Implementation of this logic expression (with a fluorescence enhancement of 12.1 between high and coincident low states) is shown in Figure 10, whilst Table 8 contains the corresponding truth table.

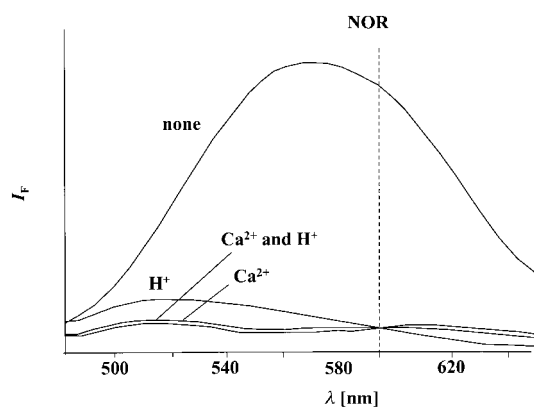


Figure 10. NOR logic with **4** through fluorescence output (excitation at 435 nm and observation at 595 nm).

## Conclusion

Simple measurements with a UV/Vis spectrophotometer unearth various logic functions within chromophores integrated with one or two receptors. The versatility is increased when the significant fluorescence of some of these compounds is examined. Perhaps most importantly, the multiplicity or superposition of logic configurations—the simultaneous accessibility of multiple logic functions—arises within photoactive **1–5** as a natural result of the multiplexing capability of light.

## Experimental Section

Aldehyde **6** was prepared as reported by Tsien,<sup>[29]</sup> 1,4-dimethylpyridinium iodide,<sup>[31]</sup> 1,4-dimethylquinolinium iodide<sup>[31]</sup> and 9-methylacridine<sup>[33]</sup> were prepared according to previously published procedures. <sup>1</sup>H NMR spectra were recorded on a General Electric GN-Ω 500 (500 MHz) instrument. Absorption spectra were recorded on a Perkin–Elmer Lambda 9 UV/Vis-NIR spectrometer; fluorescence emission spectra were recorded on a Perkin–Elmer LS-5B luminescence spectrometer. Infrared spectra were recorded on a Perkin–Elmer model 983G instrument. Electrospray mass spectra were recorded on a VG Quattro II Triple Quadrupole Mass Spectrometer.

**Methyl 2-[2-(2-[2-[di(2-methoxy-2-oxoethyl)amino]-5-methylphenoxy]ethoxy)(2-methoxy-2-oxoethyl)-4-[(E)-2-(1-methyl-4-pyridiniumyl)-1-ethenyl]anilino]acetate iodide (**1a**):** Compound **6** (0.50 g) and 1,4-dimethylpyridinium iodide (0.16 g) were dissolved in dry methanol (25 mL) and piperidine (8 drops) was added. After flushing the system with nitrogen, the mixture was heated under reflux for 20 h. The solvents were then removed under reduced pressure to give a red residue. This was dissolved in chloroform (40 mL), washed with dilute hydrochloric acid (4 × 25 mL) and water (25 mL), and then dried with sodium sulfate. Removal of solvent gave the crude product which was recrystallised from ethanol to give orange crystals (78%). M.p. 165.5–166.0 °C; <sup>1</sup>H NMR (500 MHz, CDCl<sub>3</sub>, 25 °C, TMS): δ = 8.51 (d, <sup>3</sup>J(H,H) = 7 Hz, 2H; Pyr-H), 8.06 (d, <sup>3</sup>J(H,H) = 7 Hz, 2H; Pyr-H), 7.69 (d, <sup>3</sup>J(H,H) = 17 Hz, 1H; Pyr-CH=CH-), 7.23 (d, <sup>3</sup>J(H,H) = 17 Hz, 1H; -CH=CH-Ar), 7.27 (s, 1H; Ar-H), 6.74 (s, 1H; Ar-H), 6.68 (d, <sup>3</sup>J(H,H) = 8 Hz, 1H; Ar-H), 6.79 (d, <sup>3</sup>J(H,H) = 8 Hz, 1H; Ar-H), 7.19 (d, <sup>3</sup>J(H,H) = 8 Hz, 1H; Ar-H), 6.70 (d, <sup>3</sup>J(H,H) = 8 Hz, 1H; Ar-H), 6.68 (d, <sup>3</sup>J(H,H) = 8 Hz, 1H; Ar-H), 4.43 (t, <sup>3</sup>J(H,H) = 5 Hz, 2H; -OCH<sub>2</sub>-), 4.32 (t, <sup>3</sup>J(H,H) = 5 Hz, 2H; -OCH<sub>2</sub>-), 4.28 (s, 3H; N<sup>+</sup>-CH<sub>3</sub>), 4.23 (s, 4H; N-CH<sub>2</sub>-), 4.15 (s, 4H; N-CH<sub>2</sub>-), 3.62 (s, 6H; OCH<sub>3</sub>), 3.60 (s, 6H; -OCH<sub>3</sub>), 2.29 (s, 3H; Ar-CH<sub>3</sub>); IR (KBr): ν̄ = 3003, 2950, 1743, 1643, 1518, 966, 881, 800, 768, 714 cm<sup>-1</sup>; ESMS: m/z (%): 664 (93) [M<sup>+</sup>], 344 (100) [M<sup>+</sup>+Na], 333 (22), 303 (25).

**2-[(Carboxymethyl)-2-(2-[2-[di(carboxymethyl)amino]-5-methylphenoxy]ethoxy)-4-[(E)-2-(1-methyl-4-pyridiniumyl)-1-ethenyl]anilino]acetic acid iodide (**1**):** Compound **1a** (100 mg) was dissolved in a mixture of concentrated hydrochloric acid-water (5:1 v/v) (2 mL) and refluxed for 2.5 h. After evaporating to dryness, the residue was dissolved in dilute base and filtered. Acidification to pH 2, gave a precipitate which was filtered to yield an orange solid. <sup>1</sup>H NMR (500 MHz, D<sub>2</sub>O, 25 °C, TMS): δ = 8.18 (brs, 2H; Pyr-H), 7.64 (brs, 2H; Pyr-H), 7.41 (d, <sup>3</sup>J(H,H) = 17 Hz, 1H; Pyr-CH=CH-), 7.10–6.95 (m, 2H; Ar-H, Pyr-CH=CH-), 6.89–6.68 (m, 5H; Ar-H), 4.22 (brs, 8H; N-CH<sub>2</sub>-), 3.99 (s, 3H; N<sup>+</sup>-CH<sub>3</sub>), 3.78 (s, 2H; O-CH<sub>2</sub>-), 3.61 (s, 2H; O-CH<sub>2</sub>-), 2.18 (s, 3H; Ar-CH<sub>3</sub>).

**Methyl 2-[2-(2-[2-[di(2-methoxy-2-oxoethyl)amino]-5-methylphenoxy]ethoxy)(2-methoxy-2-oxoethyl)-4-[(E)-2-(1-methyl-4-quinoliniumyl)-1-ethenyl]anilino]acetate iodide (**2a**):** Preparation of **2a** was carried out according to the synthesis of **1a**, substituting 1,4-dimethylpyridinium iodide with 1,4-dimethylquinolinium iodide. After removal of solvents a violet residue was obtained, which was purified by flash silica column chromatography, eluting with dichloromethane/methanol (9:1 v/v). Removal of solvents gave a dark red powder (70% yield). M.p. 142.7–144.9 °C; <sup>1</sup>H NMR (500 MHz, CDCl<sub>3</sub>, 25 °C, TMS): δ = 9.92 (d, <sup>3</sup>J(H,H) = 7 Hz, 1H; Quin-H), 8.29 (d, <sup>3</sup>J(H,H) = 7 Hz, 1H; Quin-H), 8.86 (d, <sup>3</sup>J(H,H) = 8 Hz,



1H; Quin-*H*), 7.95 (t,  $^3J(\text{H,H}) = 8$  Hz, 1H; Quin-*H*), 8.09 (t,  $^3J(\text{H,H}) = 8$  Hz, 1H; Quin-*H*), 8.07 (d,  $^3J(\text{H,H}) = 6$  Hz, 1H; Quin-*H*), 7.29 (d,  $^3J(\text{H,H}) = 15$  Hz, 1H; Quin-*CH=CH-*), 6.72 (d,  $^3J(\text{H,H}) = 15$  Hz, 1H; -*CH=CH-Ar*), 7.77 (s, 1H; Ar-*H*), 7.18 (d,  $^3J(\text{H,H}) = 8$  Hz, 1H; Ar-*H*), 6.64 (d,  $^3J(\text{H,H}) = 8$  Hz, 1H; Ar-*H*), 6.73 (s, 1H; Ar-*H*), 6.70 (d,  $^3J(\text{H,H}) = 8$  Hz, 1H; Ar-*H*), 6.80 (d,  $^3J(\text{H,H}) = 8$  Hz, 1H; Ar-*H*), 4.57 (s, 3H; N<sup>+</sup>-*CH<sub>3</sub>*), 4.46 (t,  $^3J(\text{H,H}) = 5$  Hz, 2H; O-*CH<sub>2</sub>-*), 4.32 (t,  $^3J(\text{H,H}) = 5$  Hz, 2H; O-*CH<sub>2</sub>-*), 4.23 (s, 4H; N-*CH<sub>2</sub>-*), 4.15 (s, 4H; N-*CH<sub>2</sub>-*), 3.64 (s, 6H; -*OCH<sub>3</sub>*), 3.59 (s, 6H; -*OCH<sub>3</sub>*), 2.25 (s, 3H; Ar-*CH<sub>3</sub>*); IR (KBr):  $\tilde{\nu} = 3017, 2950, 1732, 1588, 1205, 1005, 896, 859, 760, 613$  cm<sup>-1</sup>; ESMS: *m/z* (%): 714 (67) [*M*<sup>+</sup>], 369 (100) [*M*<sup>+</sup>+Na], 358 (53).

**2-((Carboxymethyl)-2-(2-[2-[di(carboxymethyl)amino]-5-methylphenoxy]ethoxy)-4-[(*E*)-2-(1-methyl-4-quinoliniumyl)-1-ethenyl]anilino)acetic acid iodide (2):** Acid hydrolysis of **2a** was carried out as described for the preparation of **1** to yield a violet solid. <sup>1</sup>H NMR (500 MHz, D<sub>2</sub>O, 25 °C, TMS):  $\delta = 8.99$  (brs, 1H; Quin-*H*), 8.65 (brs, 1H; Quin-*H*), 8.32–8.00 (m, 4H; Quin-*H* or Ar-*H*), 7.46 (brs, 2H; Quin-*H* or Ar-*H*), 7.23–6.95 (m, 6H; Quin-*H*, -*CH=CH-*, Ar-*H*), 4.42 (s, 3H; N<sup>+</sup>-*CH<sub>3</sub>*), 4.09 (brs, 4H; -*OCH<sub>2</sub>-*), 3.89 (brs, 8H; -*NCH<sub>2</sub>-*), 2.53 (s, 3H; Ar-*CH<sub>3</sub>*).

**Methyl 2-[2-(2-[2-[di(2-methoxy-2-oxoethyl)amino]-5-methylphenoxy]ethoxy)(2-methoxy-2-oxoethyl)-4-[(*E*)-2-(4-pyridyl)-1-ethenyl]anilino]acetate (3a):** Compound **3a** was prepared using a procedure adapted from Kost et al.<sup>[32]</sup> Benzoyl chloride (0.10 mL) was added dropwise to stirred, ice-cold 4-methylpyridine (1.3 mL) under a nitrogen stream, whereupon a precipitate of (4-methyl-1-pyridiniumyl)(phenyl)methanone chloride was produced. This was then allowed to warm to ambient temperature and **6** (0.80 g) was added. After flushing with nitrogen, the mixture was heated to 140 °C and a homogeneous solution was obtained. The initially yellow solution was seen to turn red quickly and was heated for a further 5 h. After cooling, the solution was dissolved in dichloromethane (40 mL) and poured onto crushed ice. The solute of the organic layer was adsorbed onto a minimum quantity of flash silica gel, and added to a short column of flash silica gel prepared with diethyl ether/petroleum ether (b.p. 40–60 °C) (2:1 v/v). After washing with diethyl ether/petroleum ether (b.p. 40–60 °C) (2:1 v/v) and then diethyl ether, the product was eluted with ethyl acetate to give a yellow solid after removal of solvents. This was recrystallised from isopropyl alcohol giving light yellow crystals (40% yield). M.p. 140.1–140.5 °C; <sup>1</sup>H NMR (500 MHz, CDCl<sub>3</sub>, 25 °C, TMS):  $\delta = 8.55$  (d,  $^3J(\text{H,H}) = 6$  Hz, 2H; Pyr-*H*), 7.33 (d,  $^3J(\text{H,H}) = 6$  Hz, 2H; Pyr-*H*), 7.21 (d,  $^3J(\text{H,H}) = 17$  Hz, 1H; Pyr-*CH=CH-*), 6.86 (d,  $^3J(\text{H,H}) = 17$  Hz, 1H; Pyr-*CH=CH-*), 6.79 (s, 1H; Ar-*H*), 7.07 (d,  $^3J(\text{H,H}) = 2$  Hz, 1H; Ar-*H*), 6.77 (d,  $^3J(\text{H,H}) = 2$  Hz, 1H; Ar-*H*), 6.76 (s, 1H; Ar-*H*), 4.34 (t,  $^3J(\text{H,H}) = 5$  Hz, 2H; O-*CH<sub>2</sub>-*), 4.29 (t,  $^3J(\text{H,H}) = 5$  Hz, 2H; O-*CH<sub>2</sub>-*), 4.19 (s, 4H; N-*CH<sub>2</sub>-*), 4.13 (s, 4H; N-*CH<sub>2</sub>-*), 3.59 (s, 6H; -*OCH<sub>3</sub>*), 3.55 (s, 6H; -*OCH<sub>3</sub>*), 2.27 (s, 3H; Ar-*CH<sub>3</sub>*); IR (KBr):  $\tilde{\nu} = 2998, 2951, 1748, 1589, 1518, 1416, 1254, 991, 817, 710, 668, 521$  cm<sup>-1</sup>; ESMS: *m/z* (%): 650 (79) [*M*<sup>+</sup>], 673 (46) [*M*<sup>+</sup>+Na], 337 (68), 326 (100).

**2-((Carboxymethyl)-2-(2-[2-[di(carboxymethyl)amino]-5-methylphenoxy]ethoxy)-4-[(*E*)-2-(4-pyridyl)-1-ethenyl]anilino)acetic acid (3):** Compound **3a** (50 mg) was dissolved in a minimum amount of THF, and potassium hydroxide (5 equiv) was added in aqueous solution (0.3 mL). The mixture was heated and methanol was added dropwise until a homogeneous solution was obtained. After refluxing for 90 min, water (3 mL) was added and the solution was heated under reflux for a further 20 min. The reaction mixture was then evaporated to dryness, yielding a red gum, dissolved in water and filtered. Concentrated hydrochloric acid was added slowly to the filtrate to a pH 2. The precipitate formed was then filtered to give an orange solid. <sup>1</sup>H NMR (500 MHz, D<sub>2</sub>O, 25 °C, TMS):  $\delta = 8.37$  (d,  $^3J(\text{H,H}) = 8$  Hz, 2H; Pyr-*H*), 7.47–7.38, 6.85–6.64 (m, 10H; Pyr-*H*, -*CH=CH-*, Ar-*H*), 4.39 (s, 4H; O-*CH<sub>2</sub>-*), 4.34 (s, 8H; N-*CH<sub>2</sub>-*), 2.21 (s, 3H; Ar-*CH<sub>3</sub>*).

**Methyl 2-[2-(2-[2-[di(2-methoxy-2-oxoethyl)amino]-5-methylphenoxy]ethoxy)(2-methoxy-2-oxoethyl)-4-[(*E*)-2-(4-quinolyl)-1-ethenyl]anilino]acetate (4a):** Compound **4a** was prepared by a procedure similar to that used for **3a**, replacing 4-methylpyridine with 4-methylquinoline. After heating at 150 °C for 4.5 h and cooling, the reaction mixture was dissolved in methanol and similarly loaded onto a minimum quantity of flash silica gel. This was added to a short column of flash silica gel prepared with diethyl ether. After washing with diethyl ether, the product was eluted with ethyl acetate. Removal of solvents gave a yellow solid, which was recrystallised from isopropyl alcohol to give bright yellow crystals (62% yield). M.p. 177.1–177.4 °C; <sup>1</sup>H NMR (500 MHz, CDCl<sub>3</sub>, 25 °C, TMS):  $\delta = 8.88$  (d,  $^3J(\text{H,H}) =$

5 Hz, 1H; Quin-*H*), 7.58 (d,  $^3J(\text{H,H}) = 5$  Hz, 1H; Quin-*H*), 8.22 (d,  $^3J(\text{H,H}) = 8$  Hz, 1H; Quin-*H*), 7.60 (t,  $^3J(\text{H,H}) = 8$  Hz, 1H; Quin-*H*), 7.72 (t,  $^3J(\text{H,H}) = 8$  Hz, 1H; Quin-*H*), 8.12 (d,  $^3J(\text{H,H}) = 8$  Hz, 1H; Quin-*H*), 7.68 (d,  $^3J(\text{H,H}) = 16$  Hz, 1H; Quin-*CH=CH-*), 7.27 (d,  $^3J(\text{H,H}) = 16$  Hz, 1H; Quin-*CH=CH-*), 7.17 (s, 1H; Ar-*H*), 7.15 (d,  $^3J(\text{H,H}) = 8$  Hz, 1H; Ar-*H*), 6.82 (d,  $^3J(\text{H,H}) = 8$  Hz, 1H; Ar-*H*), 6.70 (s, 1H; Ar-*H*), 6.69 (d,  $^3J(\text{H,H}) = 8$  Hz, 1H; Ar-*H*), 6.77 (d,  $^3J(\text{H,H}) = 8$  Hz, 1H; Ar-*H*), 4.39 (t,  $^3J(\text{H,H}) = 6$  Hz, 2H; O-*CH<sub>2</sub>-*), 4.31 (t,  $^3J(\text{H,H}) = 6$  Hz, 2H; O-*CH<sub>2</sub>-*), 4.21 (s, 4H; N-*CH<sub>2</sub>-*), 4.14 (s, 4H; N-*CH<sub>2</sub>-*), 3.62 (s, 6H; -*OCH<sub>3</sub>*), 3.57 (s, 6H; -*OCH<sub>3</sub>*), 2.27 (s, 3H; Ar-*CH<sub>3</sub>*); IR (KBr):  $\tilde{\nu} = 951, 1748, 1601, 1575, 1518, 1434, 1201, 1170, 1148, 1010, 882, 846, 817, 760, 710, 578$  cm<sup>-1</sup>; ESMS: *m/z* (%): 700 (100) [*M*<sup>+</sup>], 723 (35) [*M*<sup>+</sup>+Na], 362 (88), 351 (80).

**2-((Carboxymethyl)-2-(2-[2-[di(carboxymethyl)amino]-5-methylphenoxy]ethoxy)-4-[(*E*)-2-(4-quinolyl)-1-ethenyl]anilino)acetic acid (4):** Alkaline hydrolysis of **4a** (similar to the hydrolysis of **3a**) yielded **4**. Employing a similar work-up procedure, the product was obtained as a violet solid. <sup>1</sup>H NMR (500 MHz, D<sub>2</sub>O, 25 °C, TMS):  $\delta = 8.56$  (d,  $^3J(\text{H,H}) = 5$  Hz, 1H; Quin-*H*), 8.07 (d,  $^3J(\text{H,H}) = 8$  Hz, 1H; Quin-*H*), 7.88 (d,  $^3J(\text{H,H}) = 8$  Hz, 1H; Quin-*H*), 7.70 (t,  $^3J(\text{H,H}) = 8$  Hz, 1H; Quin-*H*), 7.54 (t,  $^3J(\text{H,H}) = 8$  Hz, 1H; Quin-*H*), 7.46 (d,  $^3J(\text{H,H}) = 5$  Hz, 1H; Quin-*H*), 7.37 (d,  $^3J(\text{H,H}) = 16$  Hz, 1H; Quin-*CH=CH-*), 7.07 (d,  $^3J(\text{H,H}) = 16$  Hz, 1H; -*CH=CH-Quin*), 7.04 (s, 1H; Ar-*H*), 6.80–6.87 (m, 5H; Ar-*H*), 4.19 (brs, 2H; O-*CH<sub>2</sub>-*), 4.10 (brs, 2H; O-*CH<sub>2</sub>-*), 3.76 (s, 4H; N-*CH<sub>2</sub>-*), 3.67 (s, 4H; N-*CH<sub>2</sub>-*), 2.29 (s, 3H; Ar-*CH<sub>3</sub>*).

**Methyl 2-[4-[(*E*)-2-(9-acridinyl)-1-ethenyl]-2-(2-[2-[di(2-methoxy-2-oxoethyl)amino]-5-methylphenoxy]ethoxy)(2-methoxy-2-oxoethyl)anilino]acetate (5a):** Compound **5a** was prepared according to the procedure used for **3a**; using benzoyl chloride (0.05 mL), 9-methylacridine (0.07 g) and acetic anhydride (1.5 mL). After cooling the reaction mixture it was dissolved in dichloromethane (30 mL) and poured onto crushed ice. The solute of the organic phase was then loaded onto a minimum quantity of flash silica gel and added to a short column of flash silica gel prepared with diethyl ether/petroleum ether (b.p. 40–60 °C) (3:2 v/v). After washing with diethyl ether/petroleum ether (b.p. 40–60 °C) (3:2 v/v) and diethyl ether, the product was eluted with diethyl ether/ethyl acetate (1:1 v/v). Removal of solvents gave a bright yellow powder, which was recrystallised from ethanol to give orange crystals (70% yield). M.p. 157.1–159.8 °C; <sup>1</sup>H NMR (500 MHz, CDCl<sub>3</sub>, 25 °C, TMS):  $\delta = 8.32$  (d,  $^3J(\text{H,H}) = 9$  Hz, 2H; Acr-*H*), 8.23 (d,  $^3J(\text{H,H}) = 9$  Hz, 2H; Acr-*H*), 7.52 (t,  $^3J(\text{H,H}) = 8$  Hz, 2H; Acr-*H*), 7.77 (t,  $^3J(\text{H,H}) = 8$  Hz, 2H; Acr-*H*), 7.75 (d,  $^3J(\text{H,H}) = 16$  Hz, 1H; Acr-*CH=CH-*), 6.97 (d,  $^3J(\text{H,H}) = 16$  Hz, 1H; -*CH=CH-Ar*), 7.24 (s, 1H; Ar-*H*), 7.20 (d,  $^3J(\text{H,H}) = 8$  Hz, 1H; Ar-*H*), 6.88 (d,  $^3J(\text{H,H}) = 8$  Hz, 1H; Ar-*H*), 6.71 (s, 1H; Ar-*H*), 6.68 (d,  $^3J(\text{H,H}) = 8$  Hz, 1H; Ar-*H*), 6.77 (d,  $^3J(\text{H,H}) = 8$  Hz, 1H; Ar-*H*), 4.41 (t,  $^3J(\text{H,H}) = 5$  Hz, 2H; O-*CH<sub>2</sub>-*), 4.32 (t,  $^3J(\text{H,H}) = 5$  Hz, 2H; O-*CH<sub>2</sub>-*), 4.24 (s, 4H; N-*CH<sub>2</sub>-*), 4.16 (s, 4H; N-*CH<sub>2</sub>-*), 3.63 (s, 6H; -*OCH<sub>3</sub>*), 3.59 (s, 6H; -*OCH<sub>3</sub>*), 2.27 (s, 3H; Ar-*CH<sub>3</sub>*); IR (KBr):  $\tilde{\nu} = 2951, 1746, 1626, 1517, 1435, 1250, 1201, 1167, 1011, 810, 753, 713, 602$  cm<sup>-1</sup>; ESMS: *m/z* (%): 750 (83) [*M*<sup>+</sup>], 387 (100) [*M*<sup>+</sup>+Na], 376 (48).

**2-(4-((*E*)-2-(9-Acridinyl)-1-ethenyl)(carboxymethyl)-2-(2-(2-(dicarboxymethylamino)-5-methylphenoxy)ethoxy)anilino)acetic acid (5):** Alkaline hydrolysis of **5a** (similar to the hydrolysis of **3a**) yielded **5**. Employing a similar work-up procedure, the product was obtained as a red solid. <sup>1</sup>H NMR (500 MHz, D<sub>2</sub>O, 25 °C, TMS):  $\delta = 7.84$  (d,  $^3J(\text{H,H}) = 8$  Hz, 2H; Acr-*H*), 7.78 (d,  $^3J(\text{H,H}) = 8$  Hz, 2H; Acr-*H*), 7.64 (t,  $^3J(\text{H,H}) = 8$  Hz, 2H; Acr-*H*), 7.28 (t,  $^3J(\text{H,H}) = 8$  Hz, 2H; Acr-*H*), 7.00 (d,  $^3J(\text{H,H}) = 16$  Hz, 1H; Acr-*CH=CH-*), 6.87 (d,  $^3J(\text{H,H}) = 6$  Hz, 1H; Ar-*H*), 6.67–6.77 (m, 5H; Ar-*H*), 6.46 (d,  $^3J(\text{H,H}) = 16$  Hz, 1H; -*CH=CH-Acr*), 4.23 (brs, 2H; O-*CH<sub>2</sub>-*), 4.12 (brs, 2H; O-*CH<sub>2</sub>-*), 3.75 (s, 4H; N-*CH<sub>2</sub>-*), 3.65 (s, 4H; N-*CH<sub>2</sub>-*), 2.21 (s, 3H; Ar-*CH<sub>3</sub>*).

## Acknowledgement

We thank the Department of Employment and Learning in Northern Ireland, the European Community (HPRN-CT-2000-00029) and Dr. C. Hardacre for their support and Dr. W. D. J. A. Norbert for valuable discussions.

[1] Reviews: A. P. de Silva, N. D. McClenaghan, C. P. McCoy, in *Electron Transfer in Chemistry* (Ed.: V. Balzani), Wiley-VCH, Weinheim, 2001.

- Vol. 5: Molecular-level Electronics, Imaging and Information, Energy and Environment* (Eds.: V. Balzani, A. P. de Silva, I. R. Gould), p. 156–185; A. P. de Silva, N. D. McClenaghan, C. P. McCoy, In *Molecular Switches* (Ed.: B. L. Feringa), Wiley-VCH, Weinheim, **2001**, p. 339–361; F. M. Raymo, *Adv. Mater.* **2002**, *14*, 401–414.
- [2] V. Balzani, A. Credi, F. M. Raymo, J. F. Stoddart, *Angew. Chem.* **2000**, *112*, 3486–3531; *Angew. Chem. Int. Ed.* **2000**, *39*, 3348–3391; J. P. Collin, C. Dietrich-Buchecker, P. Gavina, M. C. Jimenez-Molero, J.-P. Sauvage, *Acc. Chem. Res.* **2001**, *34*, 477–487; V. Amendola, L. Fabbrizzi, C. Mangano, P. Pallavicini, *Acc. Chem. Res.* **2001**, *34*, 488–493.
- [3] *Molecular Electronic Devices* (Eds.: F. L. Carter, R. E. Siatkowski, H. Wohltjen), Elsevier, Amsterdam, **1988**.
- [4] R. R. Birge, in *Nanotechnology; Research and Perspectives* (Eds.: B. C. Crandall, B. C. Lewis), MIT Press, Cambridge, MA, **1992**, p. 149–170.
- [5] U. P. Wild, S. Bernet, B. Kohler, A. Renn, *Pure Appl. Chem.* **1992**, *64*, 1335–1342.
- [6] A. P. de Silva, H. Q. N. Gunaratne, C. P. McCoy, *Nature* **1993**, *364*, 42–44.
- [7] S. Brasselet, W. E. Moerner, *Single Molecules* **2000**, *1*, 17–23.
- [8] R. A. Bissell, A. P. de Silva, H. Q. N. Gunaratne, P. L. M. Lynch, G. E. M. Maguire, K. R. A. S. Sandanayake, *Chem. Soc. Rev.* **1992**, *21*, 187–195.
- [9] A. P. de Silva, H. Q. N. Gunaratne, C. P. McCoy, *J. Am. Chem. Soc.* **1997**, *119*, 7891–7892.
- [10] Recent examples: A. Roque, F. Pina, S. Alves, R. Ballardini, M. Maestri, V. Balzani, *J. Mater. Chem.* **1999**, *9*, 2265–2269; L. Gobbi, P. Seiler, F. Diederich, *Angew. Chem.* **1999**, *111*, 737–740; *Angew. Chem. Int. Ed.* **1999**, *38*, 674–678; C. D. Mao, T. H. LaBean, J. H. Reif, N. C. Seeman, *Nature* **2000**, *407*, 493–496; G. McSkimming, J. H. R. Tucker, H. Bouas-Laurent, J.-P. Desvergne, *Angew. Chem.* **2000**, *112*, 2251–2253; *Angew. Chem. Int. Ed.* **2000**, *39*, 2167–2169; K. Rurack, A. Koval'chuk, J. L. Bricks, J. L. Slominskii, *J. Am. Chem. Soc.* **2001**, *123*, 6205–6206; L. Gobbi, P. Seiler, F. Diederich, V. Gramlich, C. Boudon, J. P. Gisselbrecht, M. Gross, *Helv. Chim. Acta* **2001**, *84*, 743–777; A. Ambroise, R. W. Wagner, P. D. Rao, J. A. Riggs, P. Hascoat, J. R. Diers, J. Seth, R. K. Lammi, D. F. Bocian, D. Holten, J. S. Lindsey, *Chem. Mater.* **2001**, *13*, 1023–1034.
- [11] T. Gunnlaugsson, D. A. MacDonaill, D. Parker, *Chem. Commun.* **2000**, 93–94.
- [12] K. Rurack, A. Koval'chuk, J. L. Bricks, J. L. Slominski, *J. Am. Chem. Soc.* **2001**, *123*, 6205–6206.
- [13] S. Alves, F. Pina, M. T. Albelda, E. Garcia-Espana, C. Soriano, S. V. Luis, *Eur. J. Inorg. Chem.* **2001**, 405–412.
- [14] F. M. Raymo, S. Giordani, *Org. Lett.* **2001**, *3*, 1833–1836; F. M. Raymo, S. Giordani, *J. Am. Chem. Soc.* **2001**, *123*, 4651–4652; F. M. Raymo, S. Giordani, *J. Am. Chem. Soc.* **2002**, *124*, 2004–2007; F. M. Raymo, *Adv. Mater.* **2002**, *14*, 401–414.
- [15] a) H.-F. Ji, R. Dabestani, G. M. Brown, *J. Am. Chem. Soc.* **2000**, *122*, 9306–9307; b) H. T. Baytekin, E. U. Akkaya, *Org. Lett.* **2000**, *2*, 1725–1727.
- [16] T. H. Zhang, C. P. Zhang, G. H. Fu, Y. D. Li, L. Q. Gu, G. Y. Zhang, Q. W. Song, B. Parsons, R. R. Birge, *Opt. Eng.* **2000**, *39*, 527–534; A. S. Lukas, P. J. Bushard, M. R. Wasielewski, *J. Am. Chem. Soc.* **2001**, *123*, 2440–2441; F. Remacle, S. Speiser, R. D. Levine, *J. Phys. Chem. B* **2001**, *105*, 5589–5591; F. M. Raymo, S. Giordani, *Proc. Natl. Acad. Sci. USA* **2002**, *99*, 4941–4944.
- [17] J. M. Tour, in *Stimulating Concepts in Chemistry* (Eds.: F. Vögtle, J. F. Stoddart, M. Shibasaki), Wiley-VCH, Weinheim, **2000**, p. 237–253; H. Park, J. Park, A. K. L. Lim, E. H. Anderson, A. P. Alivisatos, P. L. McEuen, *Nature* **2000**, *407*, 57–60.
- [18] C. P. Collier, E. W. Wong, M. Belohradsky, F. M. Raymo, J. F. Stoddart, P. J. Kuekes, R. S. Williams, J. R. Heath, *Science* **1999**, *285*, 391–394; C. P. Collier, G. Mattersteig, E. W. Wong, Y. Luo, K. Beverly, J. Sampaio, F. M. Raymo, J. F. Stoddart, J. R. Heath, *Science* **2000**, *289*, 1172–1175; A. R. Pease, J. O. Jeppesen, J. F. Stoddart, Y. Luo, C. P. Collier, J. R. Heath, *Acc. Chem. Res.* **2001**, *34*, 433–444.
- [19] V. Dericke, R. Martel, J. Appenzeller, P. Avouris, *Nano Lett.* **2001**, *1*, 453–456.
- [20] J. R. Lakowicz, *Principles of Fluorescence Spectroscopy*, 2nd ed., Plenum, New York, **1999**; B. Valeur, *Molecular Fluorescence*, Wiley-VCH, Weinheim, **2001**.
- [21] A. P. de Silva, H. Q. N. Gunaratne, T. Gunnlaugsson, A. J. M. Huxley, C. P. McCoy, J. T. Rademacher, T. E. Rice, *Chem. Rev.* **1997**, *97*, 1515–1566.
- [22] W. E. Moerner, T. Basche, *Angew. Chem.* **1993**, *105*, 537–557; *Angew. Chem. Int. Ed. Engl.* **1993**, *32*, 457–476; R. Bornemann, E. Thiel, *Abstr. VI Int. Conf. Meth. Appl. Fluoresc. Spectrosc.* Paris, **1999**, P7.
- [23] *Indicators* (Ed.: E. Bishop), Pergamon Press, London, **1972**.
- [24] E. B. Sandell, *Colorimetric Determination of Traces of Metals*, Interscience, New York, **1959**.
- [25] A. Ringbom, *Complexation in Analytical Chemistry*, Interscience, New York, **1963**.
- [26] *Supramolecular Photochemistry* (Ed.: V. Balzani), Reidel, Dordrecht, **1987**; V. Balzani, F. Scandola, *Supramolecular Photochemistry*, Ellis-Horwood, Chichester, **1991**; *Transition Metals in Supramolecular Chemistry* (Eds.: L. Fabbrizzi, L. Poggi), Kluwer, Dordrecht, **1994**; J.-M. Lehn, *Supramolecular Chemistry*, VCH, Weinheim, **1995**.
- [27] R. Y. Tsien, *Biochemistry* **1980**, *19*, 2396–2404.
- [28] J. van Gent, E. J. R. Sudhölter, P. V. Lambeck, T. J. A. Popma, G. J. Gerritsma, D. N. Reinhoudt, *J. Chem. Soc. Chem. Commun.* **1988**, 893–895; J. Bourson, B. Valeur, *J. Phys. Chem.* **1989**, *93*, 3871–3876; I. K. Lednev, R. E. Hester, J. N. Moore, *J. Chem. Soc. Faraday Trans.* **1997**, *93*, 1551–1558.
- [29] G. Grynkiewicz, M. Poenie, R. Y. Tsien, *J. Biol. Chem.* **1985**, *260*, 3440–3450.
- [30] L. Horwitz, *J. Chem. Soc.* **1956**, 1039–1044.
- [31] E. Klinsberg, *Pyridine and its derivatives*, Part 2, Interscience, New York, **1961**.
- [32] A. N. Kost, A. K. Sheinkman, A. N. Rozenberg, *Zh. Obshch. Khim.* **1964**, *34*, 4046–4049.
- [33] A. A. Khalaf, A. M. A. El-Khawaga, *Rev. Roum. Chim.* **1981**, *26*, 739–753.
- [34] J. T. Gerig, P. Singh, L. A. Levy, R. E. London, *J. Inorg. Biochem.* **1987**, *31*, 113–121.
- [35] A. P. de Silva, H. Q. N. Gunaratne, P. L. M. Lynch, A. L. Patty, G. L. Spence, *J. Chem. Soc. Perkin Trans. 2* **1993**, 1611–1616.
- [36] J. Millman, A. Grabel, *Microelectronics*, McGraw-Hill, London, **1988**; A. P. Malvino, J. A. Brown, *Digital Computer Electronics*, 3rd ed., Glencoe, Lake Forest, **1993**.
- [37] D. G. Cory, A. F. Fahmy, T. F. Havel, *Proc. Natl. Acad. Sci. USA* **1997**, *94*, 1634–1639; N. A. Gershenfeld, I. L. Chuang, *Science* **1997**, *275*, 350–356.
- [38] A. M. Rincon in *Encyclopedia of Electrical and Electronic Engineering Online* (Ed.: J. Webster), Wiley, New York, **1999**, article on “Logic Arrays”.
- [39] G. Hennrich, H. Sonnenschein, U. Resch-Genger, *J. Am. Chem. Soc.* **1999**, *121*, 5073–5074; G. Hennrich, W. Walther, U. Resch-Genger, H. Sonnenschein, *Inorg. Chem.* **2001**, *40*, 641–644.
- [40] G. Deng, T. Sakaki, S. Shinkai, *J. Polym. Sci. Polym. Chem.* **1993**, *31*, 1915–1920.
- [41] G. S. Cox, N. J. Turro, N. C. Yang, M. J. Chen, *J. Am. Chem. Soc.* **1984**, *106*, 422–424.
- [42] S. Nishizawa, N. Watanabe, T. Uchida, N. Teramae, *J. Chem. Soc. Perkin Trans. 2* **1999**, 141–143.
- [43] H. Bouas-Laurent, A. Castellán, M. Daney, J.-P. Desvergne, G. Guinand, P. Marsau, M. N. Riffaud, *J. Am. Chem. Soc.* **1986**, *108*, 315–317.
- [44] R. Ballardini, V. Balzani, A. Credi, M. T. Gandolfi, F. Kotzbyba-Hibert, J.-M. Lehn, L. Prodi, *J. Am. Chem. Soc.* **1994**, *116*, 5741–5746.
- [45] A. Credi, *Ph.D. Thesis*, University of Bologna, **1998**.
- [46] N. D. McClenaghan, *Ph.D. Thesis*, Queen's University of Belfast, **2000**.
- [47] D. Parker, K. Senanayake, J. A. G. Williams, *Chem. Commun.* **1997**, 1777–1778.
- [48] B. Valeur, I. Leray, *Coord. Chem. Rev.* **2000**, *205*, 3–40.
- [49] M. S. A. Abdel-Mottaleb, A. M. K. Sherif, L. F. M. Ismaiel, F. C. De Schryver, M. A. Van der Auweraer, *J. Chem. Soc. Faraday Trans. 2* **1989**, *85*, 1779–1788; K. Y. Law, *Chem. Phys. Lett.* **1980**, *75*, 545–549; B. Wandelt, P. Turkewitsch, B. R. Stranix, G. D. Darling, *J. Chem. Soc. Faraday Trans. 2* **1995**, *91*, 4199–4205.
- [50] S. L. Wang, T. I. Ho, *Chem. Phys. Lett.* **1997**, *268*, 434–438.
- [51] W. Klopffer, *Adv. Photochem.* **1977**, *10*, 311–367.
- [52] J. Rebeck, *Acc. Chem. Res.* **1984**, *17*, 258–264; P. D. Beer, A. S. Rothin, *J. Chem. Soc. Chem. Commun.* **1988**, 52–53; T. Nabeshima, T. Inaba,

- N. Furukawa, T. Hosoya, Y. Yano, *Inorg. Chem.* **1993**, *32*, 1407–1416;  
C. A. Gleave, I. O. Sutherland, *J. Chem. Soc. Chem. Commun.* **1994**,  
1873–1874.
- [53] A. P. de Silva, N. D. McClenaghan, *J. Am. Chem. Soc.* **2000**, *122*,  
3965–3966.
- [54] H. Lindauer, P. Czerney, U.-W. Grummt, *J. Prakt. Chem.* **1994**, *336*,  
521–524.
- [55] A. Credi, V. Balzani, S. J. Langford, J. F. Stoddart, *J. Am. Chem. Soc.*  
**1997**, *119*, 2679–2681.
- [56] F. Pina, M. J. Melo, M. Maestri, P. Passaniti, V. Balzani, *J. Am. Chem.*  
*Soc.* **2000**, *122*, 4496–4498.
- [57] M. Asakawa, P. R. Ashton, V. Balzani, A. Credi, G. Mattersteig, O. A.  
Matthews, M. Montalti, N. Spencer, J. F. Stoddart, M. Venturi, *Chem.*  
*Eur. J.* **1997**, *3*, 1992–1996.
- [58] a) A. P. de Silva, I. M. Dixon, H. Q. N. Gunaratne, T. Gunnlaugsson,  
P. R. S. Maxwell, T. E. Rice, *J. Am. Chem. Soc.* **1999**, *121*, 1393–1394;  
b) J.-E. Sohma Sohma, P. Jaumier, F. Fages, *J. Chem. Res.* **1999**, 134–  
135.
- [59] M. D. P. De Costa, A. P. de Silva, S. T. Pathirana, *Can. J. Chem.* **1987**,  
*65*, 1416–1419.
- [60] W. Rettig, *Top. Curr. Chem.* **1994**, *169*, 253–299.

Received: May 14, 2002 [F4089]